GEOPHYSICS, VOL. 68, NO. 2 (MARCH-APRIL 2003); P. 523–534, 9 FIGS., 1 TABLE.
10.1190/1.1567220

A quantitative appraisal of airborne and ground-based transient electromagnetic (TEM) measurements in Denmark

Anders Vest Christiansen* and Niels Bøie Christensen*

ABSTRACT

The last decade has seen growing use of ground-based transient electromagnetic (TEM) methods in Denmark for hydrogeological purposes. Due to an intensified mapping campaign, airborne TEM methods were proposed as a possible tool for mapping large areas. The first test flights were flown in June 2000 using the GEOTEM system.

Traditional approximate interpretation tools for airborne data are insufficient in hydrogeological investigations where a quantitative model specifying model parameter reliability is needed. We have carried out full nonlinear one-dimensional inversion on the field amplitude of airborne synthetic and field data and compared the airborne method with the traditional ground-based PROTEM 47 system that has found extensive use in Denmark. An improved measuring procedure for airborne systems is suggested to facilitate the estimation of noise that is necessary in a quantitative inversion.

The analyses of synthetic data demonstrate the differences in resolution capability between ground-based and airborne data. Ground-based data typically resolve three- or four-layer models and occasionally up to five layers. Airborne data resolve three layers as a maximum, one or two layers being common. The airborne GEOTEM system detects layers to depths of more than 300 m, bearing only little information about the top 50–70 m. The ground-based PROTEM 47 system has a maximum penetration of approximately 170 m, with higher resolution capabilities in the top 100 m.

Coupling to man-made conductors is a serious problem for all TEM methods in densely populated areas and results in distorted data. Coupling influences the airborne data from Denmark on two-thirds of the area covered. These data must be eliminated to avoid misinterpretation.

INTRODUCTION

The last decade has seen growing use of geophysical methods for general geological mapping purposes as well as for detailed mapping of the extent and vulnerability of aquifers (Fitterman and Stewart, 1986; McNeill, 1990; Christensen and Sørensen, 1998). Two ground-based methods have proved particularly useful in Denmark: transient electromagnetic (TEM) soundings and geoelectrical sounding/profiling. The most widely used geoelectrical methods employ the systems of continuous vertical electrical sounding with multielectrode systems (CVES) and the pulled-array continuous vertical electrical sounding system (PA-CVES) (Sørensen, 1995), which have been employed mainly for near-surface mapping to determine aquifer vulnerability. The TEM method is primarily used for delineating the lower boundary of aquifers, and more than 30,000 soundings have been made in Denmark for this purpose (Poulsen and Christensen, 1998). Recently, a pulled-array continuous TEM (PA-TEM) system has been developed allowing much faster data acquisition (Sørensen et al., 2000).

Through an agreement between the Danish counties and the national government, it was decided to map more than 20 000 km^2 (about half the area of Denmark) over the next decade using geophysical methods to obtain a thorough knowledge of the groundwater resources. The estimated total cost is US$100 million, financed through water taxes, a project unique in both intention and proportions.

The project scope has drawn attention to the requisite geophysical methods. The continuous PA-TEM system is much faster than a single site stationary system, but is still insufficient for a project of this size, and airborne TEM methods, which offer high efficiency, have been proposed.

Published on Geophysics Online November 15, 2002. Manuscript received by the Editor June 26, 2001; revised manuscript received May 14, 2002.
*University of Aarhus, Department of Earth Sciences, Finlandsgade 8, 8200 Åarhus N, Denmark. E-mail: anders.vest@geo.au.dk; nbc@geo.au.dk.

Airborne TEM methods

Airborne TEM methods have traditionally been used in mineral exploration for mapping highly conductive bodies in a resistive background (Pedersen and Thompson, 1991; Smith and Keating, 1996), with qualitative more than quantitative purposes. One-dimensional imaging techniques have so far been the most abundant tools for processing of the airborne data, and several techniques have been suggested based on the variation of the diffusion velocity with conductivity (DeMoully and Becker, 1984; Macnae and Lamontagne, 1987; Macnae et al., 1991; Liu and Asten, 1993). These algorithms find the depth to an equivalent current filament as a function of time, from which the diffusion velocity and thereby the conductivity can be found. The conductivity is then ascribed to a depth equal to the image depth scaled with an ad hoc factor to produce the best results. The conductivity-depth transform (CDT) by Wolfgram and Karlik (1995) belongs to the group of methods mentioned above, and is used by Fugro Airborne surveys as a standard tool for interpretation of data from the widely used GEOTEM system.

The CDT deconvolves the measured data with respect to the system response to produce the step response (repeated with alternating polarity). Based on the simplifying assumption that the step response of the earth can be represented as a series expansion into decaying exponential functions with different time constants (Stolz and Macnae, 1998), the measured data are expressed in terms of these basis functions convolved with the system response. A system of linear equations is then solved for the amplitudes of the basis functions. The deconvolution is nonunique and depends on the range and number of time constants preselected for the exponentials. This method results in smooth pictures of the subsurface conductivity.

However, the usefulness of a groundwater investigation in a sedimentary environment is substantially enhanced with a quantitative output model including quantitative analyses of model resolution (Christensen et al., 2000). We present a full nonlinear inversion scheme, producing 1D layered earth models with a quantitative analysis of resolution. Instead of the inherently unstable deconvolution of data, the inversion convolves the 1D model response with the transmitter waveform, which is a stable process (Christensen, 2002). This technique is related to the Liu and Asten (1993) convolution.

We compare airborne and traditional ground-based TEM methods. The study involves both synthetic models and field case studies. The flight lines presented are part of the first airborne TEM project carried out in Denmark in Ringkjøbing County. The system used was the GEOTEM system from Fugro Airborne Surveys Ltd. The ground-based system used for comparison is the PROTEM 47 equipment from Geonics Ltd.

The field area

The field area is characterized by Quaternary and Tertiary sediments to quite large depths (>300 m). The area was not covered with ice during the last glacial period [Weichsel (Europe) or Wisconsin (North America)]. Therefore, the top layers are dominated by two features: tills older than the Weichsel and fluvial deposits from the Weichsel glaciation. The Quaternary sediments vary in thickness from a few meters to more than 100 m, and are often deformed by glacial activity. The formations below the Quaternary sequence contain important aquifers in fluvial and deltaic Oligocene and Miocene deposits interbedded with mica clay. This sequence is underlain by Paleogene fine clay (Friis et al., 1998; Friborg and Thomsen, 1999). Figure 1 presents a schematic overview of the lithology in the area with approximate unit thicknesses.

METHODOLOGY

To obtain meaningful models from the inversion of TEM data and to make comparative analyses of data fit and model reliability, it is essential to specify the recording situation. Special attention must be given to system specifications and a thorough description of the noise model (Munkholm and Auken, 1996).

System specifications

System specifications are summarized in Table 1 and Figure 2.

PROTEM 47 from Geonics Ltd is a standard, single-site, ground-based system. The current source is a 40×40 m^2 loop, with the receiver coil at the center of the loop measuring the vertical component of the dB/dt field. The measurements are split in three segments each with 20 time channels (gates), distributed with 10 per decade in time.

GEOTEM from Fugro Airborne Surveys is a fixed-wing TEM system with receiver coils in a trailing bird. The loop is strung around the airplane, and the receiver consists of three mutually perpendicular induction coils measuring the three components of dB/dt. Data are sampled continuously and subsequently binned in 20 gates with only the last 15 being in the off-time (distributed between 0.2 and 4.4 ms from the end of the transmitter pulse). For a more detailed description of both

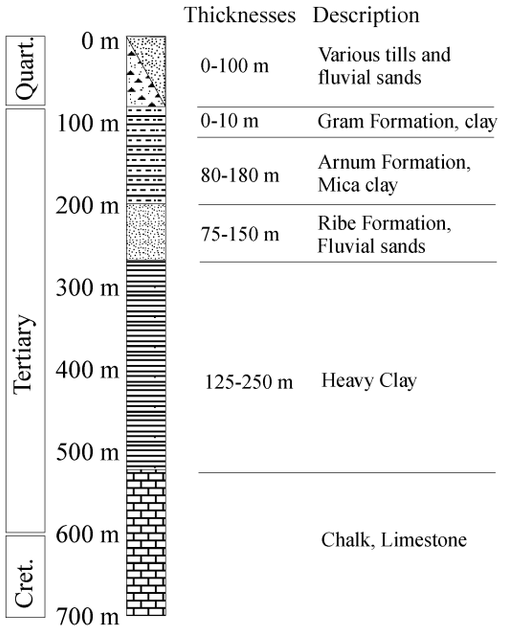

FIG. 1. Schematic representation of the lithologies in western Jutland Formations. Depths are not to scale.

the TEM method in general and various systems, see Nabighian and Macnae (1987).

Noise model

The transient data value is an averaging of the induced electromotive force in the receiver coil within the gate. Ground-based methods normally use logarithmic gating, meaning that the length of a gate is proportional to delay time. If the surrounding noise is white (i.e., stochastic through all frequencies), logarithmic gating results in an effective noise decay of $t^{-1/2}$. However, the surrounding noise is not white. The spectra of AM transmitters have high amplitudes at single frequencies. These thin spectral lines will overlay the white noise. Averaging and stacking such monochromatic signals results in an effective noise decay of t^{-1} (Christensen et al., 2000). This contribution will dominate at early times, whereas the stochastic noise will dominate at late times. In Denmark, the transition time of the PROTEM 47 system is 100 μs and the value at this delay time is 10 nV/m^2, determined through several experiments. The total absolute noise is the sum of the two contributions. Figure 3 shows the total noise as a function of time.

Standard field procedures with the GEOTEM system do not include actual measurements of the noise level because this is rather time consuming. Thus, the only way to estimate the noise on GEOTEM data is by inspecting the regular data. Assuming that the data from the last gate contain no or little signal from the earth, the standard deviation (STD) on these data can be used to estimate the noise level. The noise levels on all other off-time gates are found by scaling with the relative length of the gates:

$$\text{noise}(n) = \text{STD}(20)\sqrt{\frac{\text{length}(20)}{\text{length}(n)}} \qquad (1)$$

for the nth gate. This noise model as found from the Ringkjøbing data set is also illustrated in Figure 3. Note that all other noise sources are ignored here (i.e., roll, pitch, bird position fluctuations, etc.). The data are assigned another 5% relative noise due to the fact that the model assumption has a lower-ranking dimensionality than the targets, and to account for deviations from the nominal configuration (Smith, 2001b). The absolute noise described above and the 5% relative noise together describe the standard noise model.

The GEOTEM system measures continuously and, thus, also has on-time gates. However, the standard field procedures of high-altitude measurements are presently only aimed at determining the average waveform and does not include a statistical analysis of its variation. The primary field of the average waveform is subtracted from the measured data, and the variation

Table 1. Summary of specifications for the GEOTEM and PROTEM 47 systems.

	GEOTEM	PROTEM 47
	Transmitter (Tx)	
Area	230 m^2	1600 m^2
Max. moment	6.18×10^5 Am^2	4800 Am^2
Waveform	2 ms half-sine	square 2 μs turnoff
Duty cycle	33%	50%
	Receiver (Rx)	
Components	x, y, and z	z
Sampling	continuous 128 points per half-cycle	7 μs–7 ms from end of turnoff
Gates	20 with 15 in off-time	60 in 3 segments
	Geometry	
Tx elevation	120 m	0 m
Rx elevation	70 m	0 m
Tx-Rx dist.	131 m	0 m

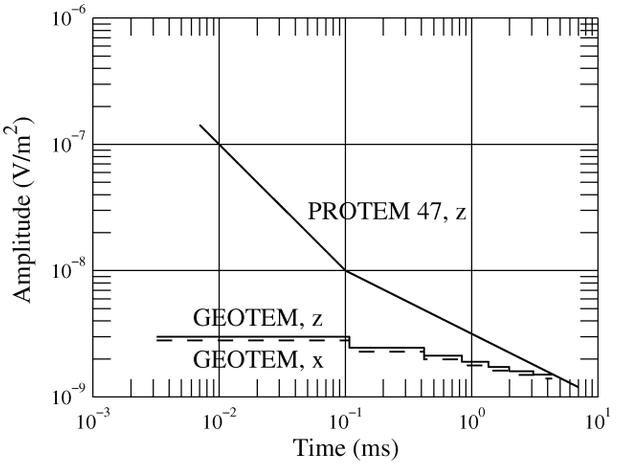

FIG. 3. The absolute noise assumed for the TEM sounding data. The length of the lines indicate the time-interval in which data are recorded, measured from the end of the transmitter pulse. The noise levels are absolute and not normalized according to the effective transmitter current. The labels x and z refer to the x and z-components of the measured dB/dt field.

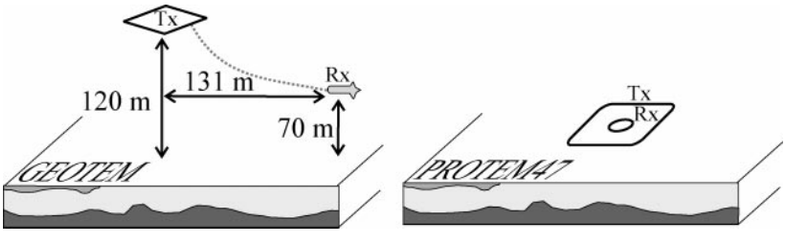

FIG. 2. Schematic representation of the PROTEM 47 and GEOTEM systems field setups.

of the primary field thus contributes to the noise, particularly on the on-time measurements. The absence of an estimate on the variation of the primary field makes it virtually impossible to estimate a noise model for on-time data. Therefore, we have focused on modeling only the off-time gates of both systems. On-time measurements are finding increasing use for various purposes (Annan et al., 1996; Smith, 2000, 2001a, Smith and Balch, 2000; Smith and Lee, 2002), and with an extended analysis of already existing field procedures, including an estimate of the variability of the primary field, the inclusion of on-time data in a full nonlinear quantitative inversion scheme is very interesting and an area of present research (Christiansen and Christensen, 2001).

Forward calculations

All modeling and inversion are done using the 1D full nonlinear inversion program SELMA (Christensen and Auken, 1992). SELMA approximates the actual geometry of the transmitter source with a circular current loop of the same area. For the airborne data, the actual height of the transmitter and receiver is taken into account. Computation of the field quantities as functions of time and space, are done through calculations in the Laplace/wavenumber domain followed by an inverse Laplace transform using the Gaver-Stehfest algorithm (Knight and Raiche, 1982) and a subsequent Hankel transform using the digital filters of Christensen (1990).

Calculation of PROTEM 47 responses includes both a waveform with turn-on and turn-off ramps, and modeling of the effect of all system band-pass filters. The characteristics of the filters were measured in the laboratory. The incorporation of the band limitation has been shown to be crucial for accuracy (Effersø et al., 1999). The band limitation is modeled by multiplication with the pertinent filter in the Laplace domain before transforming to the time domain. The actual transmitter waveform is included as a convolution in the time domain by approximating the waveform with a piecewise linear function and calculating the induction coil response as a linear combination of step response values.

The GEOTEM response, however, is calculated using the waveform convolution only. The waveform is found from the transmitter signal as measured by the receiver coils in high-altitude measurements (Figure 4).

This signal comprises all effects due to induction in the aircraft and any band-pass filtering applied through the receivers. The filtering effect of the receiver is seen as a distinct time delay in Figure 4 comparing the transmitter waveform with the waveform measured by the receiver coils. The figure also outlines the fact that the waveform used for computation is drawn to zero and truncated well before the first gate opens, in order to do off-time calculations only. At the time of this study, on-time modeling was not available, but present research includes modeling of the on-time signal as well (Christiansen and Christensen, 2001). Preliminary results suggest that the error on the first gate using the truncated waveform is approximately 2%, decreasing for the following gates. Bringing the truncation of the discretized waveform closer to the first gate makes the relative error larger. Ideally all data should of course be modeled on-time.

Inversion methodology

Two extensively used inversion types were applied: few-layer and multilayer inversion. The few-layer (or block-type) inversion we define as an inversion minimizing the data misfit using the fewest number of layers. The inversion parameters are layer thicknesses and resistivities. In the multilayer inversion (underdetermined, minimum-structure), the only parameters free to vary are the layer resistivities, the layer boundaries being kept fixed. To avoid erratic models, the inversion is regularized by claiming identity between the resistivities of neighboring layers within a certain relative uncertainty. The initial model is a homogeneous half-space, which means that no qualified guess is necessary.

The inversion is realized as an iterative damped least-squares approach (Menke, 1989), formally written as the model update at the nth iteration:

$$\mathbf{m}_{n+1} = \mathbf{m}_n + \left[\mathbf{G}_n^T \mathbf{C}_{obs}^{-1} \mathbf{G}_n + \mathbf{B}^T \mathbf{C}_c^{-1} \mathbf{B} + \lambda \mathbf{I}\right]^{-1} \cdot \cdot \left[\mathbf{G}_n^T \mathbf{C}_{obs}^{-1} (\mathbf{d}_{obs} - \mathbf{d}_n) + \mathbf{B}^T \mathbf{C}_c^{-1} (\mathbf{C}_0 - \mathbf{B}\mathbf{m}_n)\right], \quad (2)$$

where $\mathbf{m}$ denotes the model vector, $\mathbf{G}_n$ is the Jacobian matrix, $\mathbf{C}_{obs}$ is the data error covariance matrix, $\mathbf{B}$ is the roughness

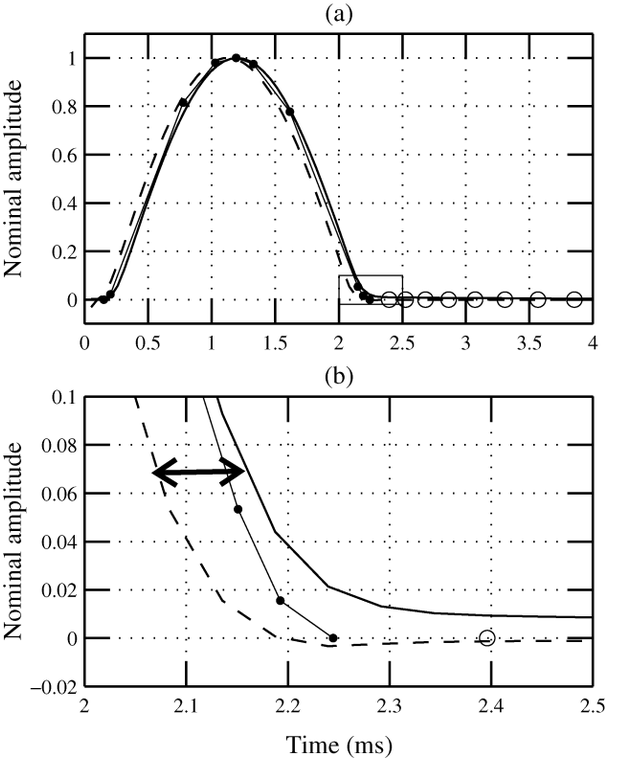

FIG. 4. The GEOTEM transmitter waveform. (a) The waveform as measured with the receiver coils (solid line) and as measured with a pick-up coil at the aircraft (dashed line). The dotted solid line is the 10-point piecewise linear waveform used for computations, and the circles mark the gate-center positions. (b) A magnification of the framed area in (a). The time delay between the transmitter waveform and the waveform picked up by the receivers is marked with the arrow in (b).

matrix containing 1 and −1 for the parameters that are tied together in the multilayer inversion, $\mathbf{C}_c$ is the the covariance matrix of the constraints between layers, λ is the damping factor, $\mathbf{I}$ is the identity matrix, $\mathbf{d}_{obs}$ is the data vector, $\mathbf{d}_n$ is the forward data vector based on the previous model vector $\mathbf{m}_n$, and finally $\mathbf{C}_0$ is a null vector claiming identity between the constrained parameters. The standard noise model enters the inversion procedure in the data covariance matrix assuming uncorrelated Gaussian noise.

The model parameter analysis is based on a linear approximation to the covariance of the estimation error, $\mathbf{C}_{est}$ (Menke, 1989):

$$\mathbf{C}_{est} = \left(\mathbf{G}^T \mathbf{C}_{obs}^{-1} \mathbf{G}\right)^{-1}, \tag{3}$$

where $\mathbf{G}$ is based on the final model obtained in the inversion.

Inversion is carried out in the the log(data)-log(parameter) space, and the data fit is determined by the residual, RES, given by

$$RES = \sqrt{\frac{1}{N}\sum_{n=1}^{N}\frac{(y_n - d_n)^2}{\sigma_n^2}}, \tag{4}$$

where d_n denotes the observed data, y_n denotes the predicted data, σ_n denotes the standard deviation, and N is the number of data points.

The field amplitude data type

During flight, the receiver bird position varies (Smith, 2001b), and the motions tend to mix the three components of the measured field, so that dB_x/dt contains some dB_z/dt and dB_y/dt, and correspondingly for the other components. To deal with this problem, it is advantageous to introduce a new data type called the field amplitude (FA) (e.g., Poulsen, 2000), defined as

$$FA = \sqrt{\frac{dB_x^2}{dt} + \frac{dB_y^2}{dt} + \frac{dB_z^2}{dt}}, \tag{5}$$

where dB_x/dt, dB_y/dt, and dB_z/dt are the measured time derivatives of the components of the magnetic field. Figure 5a presents a small section of three selected channels (early time, intermediate time and late time) from the field data. The oscillating character of the x- and z-component data are caused by the receiver bird motions. The FA data type eliminates to a large extent the effects of receiver bird movements.

Figure 5b is the result of an inversion on one sounding (indicated by the dashed line in Figure 5a) using the FA data type. The predicted data fit the observed with a residual of 0.07 [equation (4)]. Figures 5b and 5c illustrates the problem with a joint inversion of the x- and z-components. Compared with the predicted data, the x-component data are too high and the z-component data are too small, giving a misleading outcome of the joint inversion with a residual of 1.6. The main reason to use the FA data type is the reduction of the effects of receiver bird motion, but additional advantages are achieved:

1) The FA enables inversion on raw data, which means less lateral smoothing, reducing the effects of coupling to man-made conductors as much as possible (see later section).
2) The FA is less affected by possible 2D effects on a sublayered half-space. This is due to the fact that the lateral character of the FA sensitivity function is smooth, whereas the x- and z-component sensitivity functions are very different (Christiansen and Christensen, 2000), inevitably disrupting a joint inversion in the presence of 2D structures.

We will base all interpretations and analyses of airborne data on the FA data type.

SYNTHETIC EXAMPLES

The 1D earth model is in many cases inadequate to describe the complex resistivity structure of the earth, but due to the

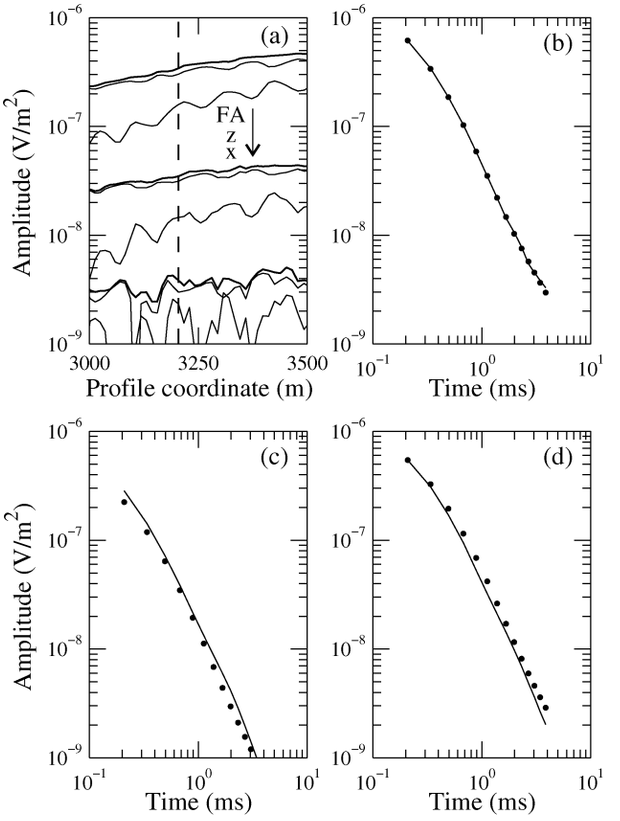

FIG. 5. The advantages of the FA data type. (a) Components x, z, and FA of channels 7, 11, and 18 from observed data are presented. (b) Predicted data (dots) compared with observed data (solid) using the FA data type for inversion. (c) Predicted x-component data (dots) from a joint inversion of the x- and z-component data and observed data (solid). (d) As (c) but for the z-component. The data shown in (b)–(d) are indicated by the vertical dashed line in (a).

prohibitively high computational costs of 2D and 3D models it is by far the most frequently used model in the interpretation of TEM data.

We have chosen to analyze two models each of which is changed in 21 steps, giving rise to 42 1D models altogether. Both central models represent important settings for hydrogeological surveys in Denmark. The models include three layers. More layers could be relevant in describing the geological setting, and the ground-based systems are in many cases able to resolve more than three layers, but this is beyond the capabilities of an airborne system (Christensen et al., 2000). The synthetic data are produced using forward calculations, and noise is ascribed using the standard noise model described above. For both systems, Figures 6 and 7 present, from top to bottom, the true models, analyses, few-layer inversions, and multilayer inversions. The five color-coded lines in the model analyses, as described in equation (3), represent the five parameters in the true three-layer model, from the top: layer resistivities (RES1, RES2, and RES3) and layer thicknesses (THK1 and THK2). The colors indicate the relative uncertainty on each parameter from well determined (red) to undetermined (blue). All the displayed models gave predicted data that fit the observations to a level appropriate to the noise introduced.

Model 1, double descending

Model 1 in Figure 6a is a double-descending model with resistivities 200 ohm-m (layer one), 70 ohm-m (layer two), and 5 ohm-m (layer three). The thickness of the first layer is 30 m. The thickness of the second layer is changed in 21 exponential steps from 3 m to 300 m (10 per decade). The layers are intended to represent a sandy top layer overlaying an aquifer (both Quaternary) and, at the bottom, a heavy Tertiary clay delineating the lower aquifer boundary.

The true-model analyses for the PROTEM 47 system (see Figure 6b) present all well-determined parameters when the thickness of the second layer is about the thickness of the first layer (Figure 6b, 10). This is the case until the second layer reaches considerable thickness (Figure 6b, 18–19). The true-model analyses for the GEOTEM system (Figure 6c) has

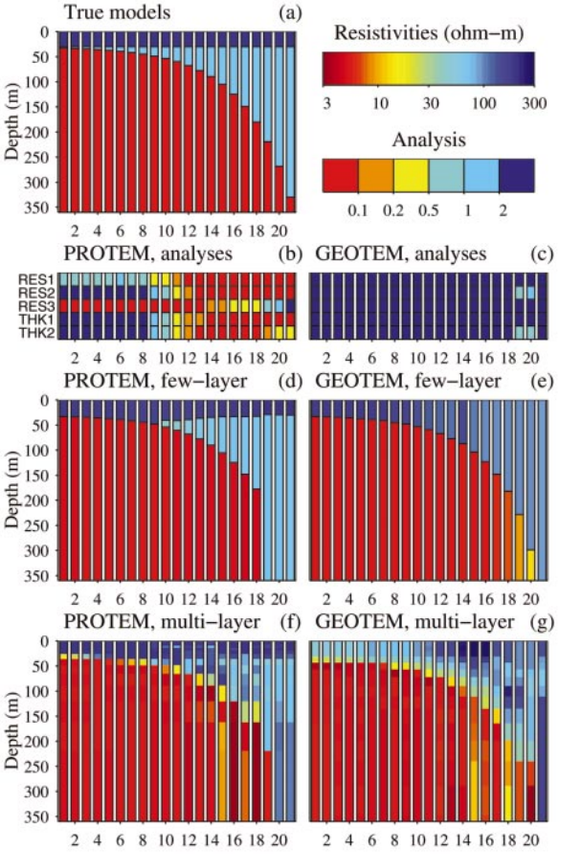

FIG. 6. Model 1: 21 double-descending 1D models. (a) True models. (b) and (c) True model analyses. (d) and (e) Few-layer inversions. (f) and (g) Multilayer inversions. PROTEM 47 on the left side, GEOTEM on the right. The colors of the analyses indicate the relative uncertainty on each parameter from well determined (red) to undetermined (blue).

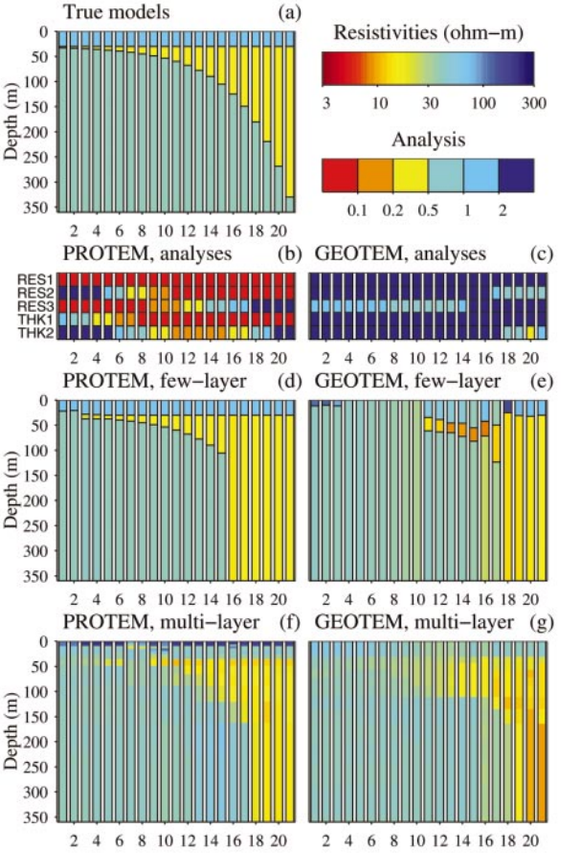

FIG. 7. Model 2: 21 low-contrast 1D models. (a) True models. (b) and (c) True model analyses. (d) and (e) Few-layer inversions. (f) and (g) Multilayer inversions. PROTEM 47 on the left side, GEOTEM on the right. The colors of the analyses indicate the relative uncertainty on each parameter from well determined (red) to undetermined (blue).

poorly determined parameters in all models, indicating that the models cannot be resolved.

The few-layer inversions for the PROTEM 47 system (Figure 6d) reflect the analysis above since all three layers are only resolved for the part where all the model parameters were well determined, but there is some problem finding the correct thicknesses and resistivities due to equivalences (Figure 6d, 10–14). The depth to the good conductor is resolved for all models until it reaches a depth of 200 m (Figure 6d, 19). The GEOTEM data (Figure 6e) are in all cases satisfactorily interpreted with a two-layer model, in agreement with the analyses. The good conductor is found for the entire depth range except the very last part where the conductor is at a depth of 330 m (Figure 6e, 21).

Only very little new information appears when the PROTEM 47 data are interpreted with multilayer models (Figure 6f), though it seems that some information about the third layer is present when it is buried at great depths (Figure 6f, 19). The GEOTEM data (Figure 6g) introduce a little information on the second layer using multilayer inversions (e.g., Figure 6g, 16–17) but, on the other hand, the top layer resistivity is erroneous at other models (Figure 6g, 1–12), indicating low resolution capability.

Model 2, low contrast

Model 2 (Figure 7a) is a low-contrast model with resistivities 70 ohm-m, 15 ohm-m, and 40 ohm-m. Again the thickness of layer one is 30 m, and the thickness of layer two is changed in 21 steps from 3 m to 300 m. In geological terms, this model could resemble a clayey and sandy Quaternary top layer overlaying a Tertiary mica clay, and a sandy aquifer at the bottom.

The true-model analyses for the PROTEM 47 inversions (Figure 7b) reflect well-determined parameters in the top layers except for a very thin (Figure 7b, 1–5) or very thick (Figure 7b, 17–21) second layer. The bottom layer is well determined for depths less than 100 m (Figure 7b, 1–14); otherwise, it is undetermined. The GEOTEM system (Figure 7c) shows mainly poorly resolved parameters, with a little information on the third layer for intermediate depths (Figure 7c, 9–13), and on the second layer for large thicknesses of this layer (Figure 7c, 19–21).

The top layers are distinguishable in most cases with the few-layer inversions on the PROTEM 47 system (Figure 7d, 3–21), whereas the bottom layer can only be distinguished until depths of approximately 100 m (Figure 7d, 15). The few-layer inversions with the GEOTEM system (Figure 7e) invert this model with a homogeneous half-space in many cases (Figure 7e, 3–10). For considerable thicknesses of the second layer, a three-layer model is necessary (Figure 7e, 11–17), but the thickness of the second layer is greatly underestimated, causing a lower resistivity due to equivalences.

The multilayer inversions on PROTEM 47 data (Figure 7f) add some information on the deeper parts of the models (Figure 7f, 16–18), whereas the second layer seems harder to recognize for small thicknesses (e.g., Figure 7f, 3–10). The GEOTEM multilayer inversions (Figure 7g) also bring some information to the deeper parts of the models (Figure 7g, 12–19), but no new information on the thickness of the second layer is introduced for the few-layer models that needed a three-layer model (Figure 7g, 11–17).

Interpretations

On the basis of the synthetic examples it can be concluded that:

1) PROTEM 47 needs three layers whenever the equivalences are not too strong, but always at least two layers, reflected by both the analyses and the few-layer interpretations.
2) GEOTEM data contain information to resolve a two-layer model in most cases, with erroneous three-layer models in some cases, again in agreement with both analyses and few-layer inversions.
3) The PROTEM 47 system resolves layers to depths of approximately 200 m in the best case, (Figure 6d, 18).
4) The GEOTEM system detects layers to depths of approximately 300 m (Figure 6e, 20).
5) The PROTEM 47 system is superior in resolving the top layers, where GEOTEM data have very limited resolution (e.g., Figures 7d and 7e, 4–10).
6) Multilayer inversion in some cases enhances information from weak signals referring to the deeper parts of the models (Figure 6f, 19).
7) For the shallower parts, the few-layer inversion seems superior to multilayer inversion (Figures 7d and 7f, 5).
8) GEOTEM data seem to gain most by multilayer inversion.

FIELD EXAMPLES

In June 2000, two test flights were flown in Denmark using the GEOTEM system from Fugro Airborne Surveys Ltd. The one addressed here was flown in Ringkjøbing Amt in western Jutland. About 500 line-km of data were collected altogether, of which we will present 25 km here. The section is chosen because ground-based data have been collected for part of the line as well. However, before presenting the results, the problem with coupling to man-made conductors needs to be addressed.

Coupling

Denmark is densely populated, and the part not covered by cities is used for agricultural purposes. This means that roads with crash barriers and buried cables, power lines, animal fences, telephone cables, etc. are ubiquitous. All these installations give rise to coupling when the primary field from the transmitter loop is imposed (Sørensen et al., 2001). This disturbance is deterministic, arising at the same delay time for all decays summed in the stacking process. A general model for the disturbance from man-made structures is that of an oscillating circuit, and is normally categorized into two types: galvanic and capacitive coupling. Figure 8 presents the two types of coupling, from the line of data to be presented below.

A galvanic-type coupling could arise from high-voltage power lines, grounded at each pylon. Animal fences and highway crash barriers are other examples. The galvanic coupling is characterized by an L-R-circuit, with the nonoscillatory decay decreasing exponentially. The disturbance depends on the time constant of the circuit, and it can be very hard to recognize on single-site soundings because the whole sounding curve is shifted. An example of a galvanic coupling from a 10-kV power line is shown for a single sounding in Figure 8a. In

a data sweep, this type of coupling can be recognized because it often looks like a response from a vertical thin sheet, as seen in Figure 8c (Smith and Keating, 1996). However, data weakly affected by galvanic coupling might be difficult to recognize in the model sections from inversions on the FA, as seen in Figure 8e, in which the coupling is only visible as a dome structure from approximately coordinate 0.4 km to 1.4 km with a smaller structure superimposed at coordinate 0.8 km. Thus, using the FA data type tends to subdue (not remove) the influence of weak galvanic coupling, because the x- and the z-component data profile have different shapes and are slightly out of phase across the coupling. Stronger galvanic coupling would inevitably disturb the model section. Because accuracy can be crucial in a ground water survey, all artificially coupled data need to be removed before the final interpretation. Figure 8g shows model section (e) without the coupled data. The footprint or trend of a galvanic coupling can be quite large as indicated by the amount of removed data, but it closely reflects the tail of the coupling in Figure 8c.

A capacitive type coupling could arise from buried polyurethane insulated cables. The capacitive coupling is characterized by an L-C-R-circuit, and the disturbance depends on the time constant and the resonance frequency of the circuit. This type of coupling is most often easily recognized because of its oscillating character as seen in Figures 8b and 8d. The data in Figure 8b are clearly not a geological response. The capacitive-type coupling is easily recognized in the model section as well (Figure 8f), in this case as an elevation of the good conductor. The effect of the coupled data is again removed in the last panel (Figure 8h). Altogether, coupling affected two-thirds of the collected data, which had to be manually identified and removed before interpretation. All the model sections from the nonlinear inversion scheme are presented without the coupled data and thus appear with large white areas in between model subsections. The remaining subsections are the parts that can be trusted and on which a meaningful interpretation can be based.

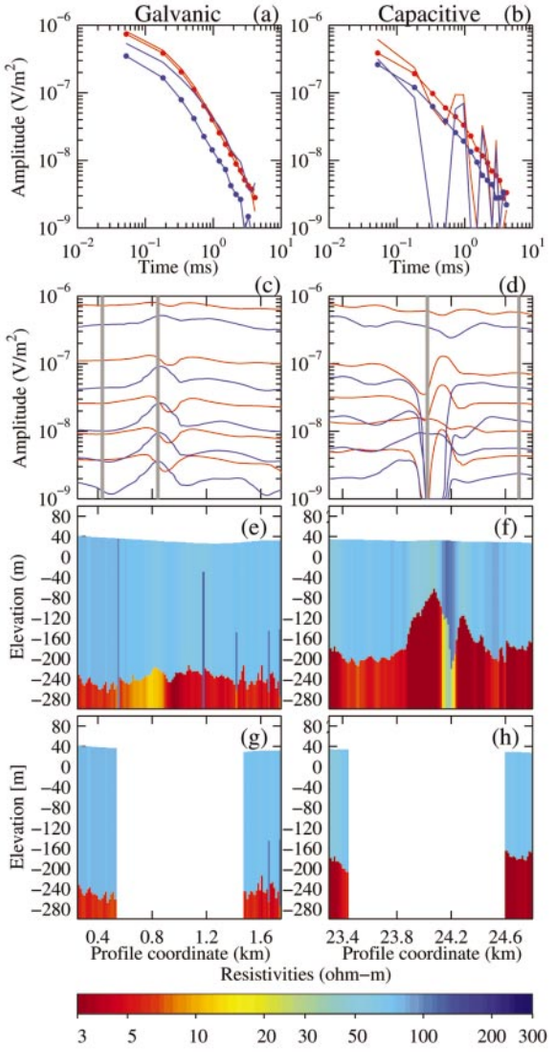

FIG. 8. Coupling to man-made conductors. (a) and (b) Coupled (solid) and uncoupled (solid, dotted) data. The blue lines are the x-component, the red lines are the z-component. Galvanic type coupling on the left, capacitive type on the right. (c) and (d) Selected gates as a data sweep along the profile. The position of the soundings displayed in (a) and (b) are indicated by the vertical gray lines. (e) and (f) Model sections from inversions on the FA. (g) and (h) The same profile without the coupled soundings.

Results

All the field data are presented in Figure 9. The flying direction is from right to left, and the reference point is the position of the receiver.

On the data sweep (Figure 9a), the enlarged sections presented in Figure 8 can be identified at profile coordinates 1 and 24 km. A number of other coupled data sets are easily identified even at this scale (e.g., at coordinates 5, 6.3, 15.2, 18, 19.5, 21.5, and 22.6 km); others are not identifiable at this scale. The feature at coordinate 3 km is caused by the aircraft rising to a height of 200 m.

The most distinctive feature in the few-layer inversion of GEOTEM data (Figure 9b) is the conductive layer at large depth, only missing around coordinate 18.5 km. The models generally need two layers to fit the data, with three layers in 29% of the models. The models from inversions of PROTEM 47 data in Figure 9c all have high resistivities with a slightly more conductive feature at the top, especially around profile coordinates 15–22 km. The data are unfortunately of very poor quality, possibly affected by the coupling also affecting the GEOTEM data at that part of the line. The data are fitted with two to five layers, but no common features seem to connect the separate soundings.

The multilayer interpretations of GEOTEM data (Figure 9d) also have the conductive layer at depth as the most distinctive feature. The layer is missing around coordinate 3 km, but this is just where the aircraft rose to 200 m with a resulting lower signal-to-noise-ratio. Again the layer is also missing at coordinate 19 km. The layers above the conductive layer appear to have more structure than indicated by the few-layer inversions. The multilayer inversions on PROTEM 47 data (Figure 9e) are very similar to the few-layer inversions, revealing no new information.

The CDT model section (Figure 9f) presents data from the whole line, including the coupled soundings. This is not possible

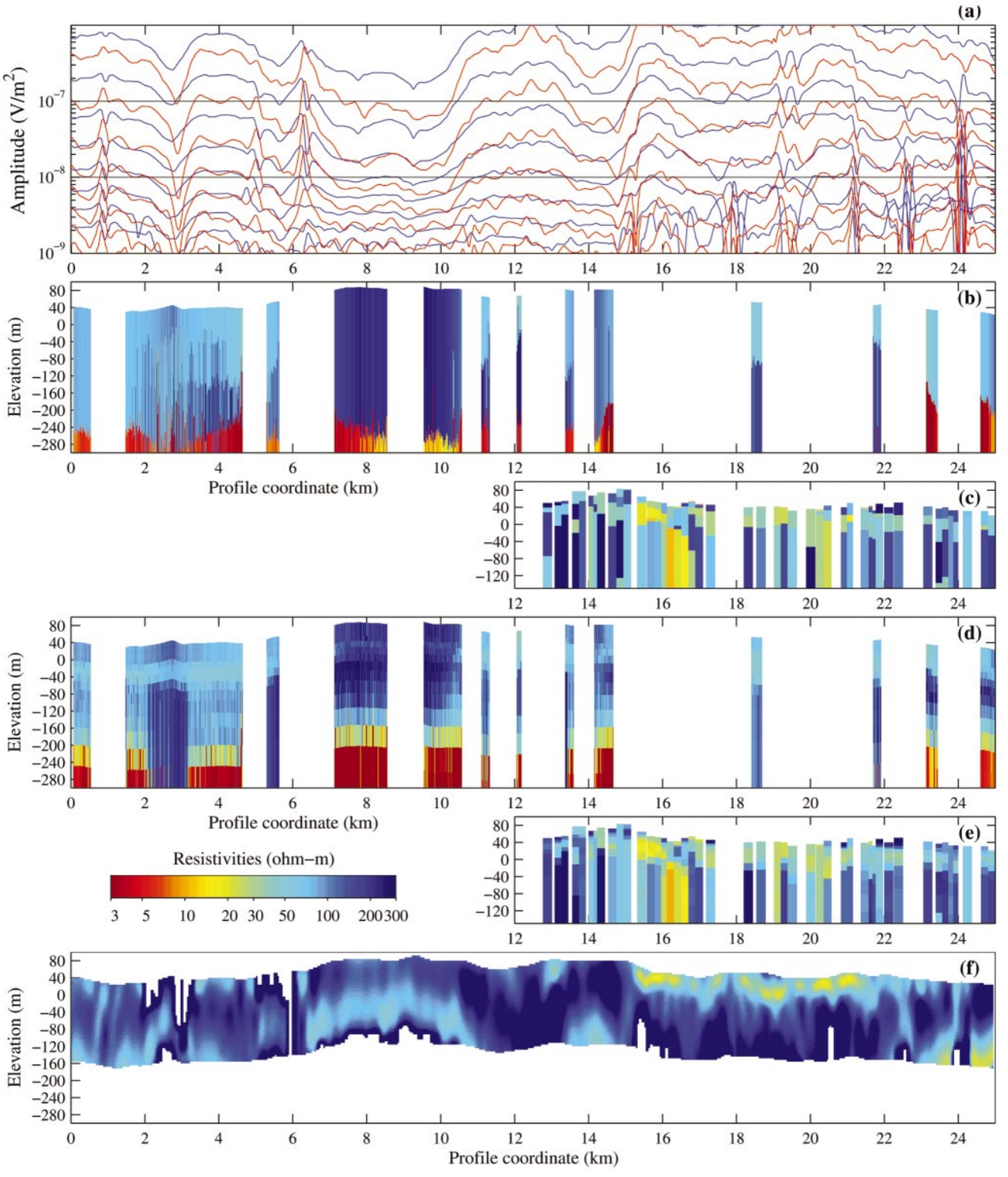

FIG. 9. Inversions of the field data. (a) Full data profile with x-component in red and z-component in blue. (b) Few-layer inversions of the airborne data in (a). (c) Few-layer inversions of PROTEM 47 data from part of the profile. (d) and (e) Inversions using a multilayer model. (f) The model obtained using the CDT inversion scheme.

without a heavy smoothing of data before processing, and two undesirable effects arise from this: (1) coupled data, and thereby unpredictably distorted models, are not identified, and (2) the lateral smoothing smears out the distortions of the coupled data to the uncoupled data sets. A number of the distinct features on the CDT profile appear in areas where the data are known to be affected by coupling. Most prominent is the conductive near-surface feature in the profile interval 16–22 km, the part of the profile with the most severely coupled data. Fugro Airborne Surveys has truncated the CDT profile at the given depth based on an estimated diffusion depth of the last datum followed by a visual evaluation of the model section. The CDT does not see the good conductor. The average resistivities found for the upper parts are similar to the resistivities found in the few-layer and multilayer sections.

Interpretations

The conductive layer at depth is interpreted to be heavy Paleogene clay known to be at that approximate depth in the area (Figure 1). Seismic sections close to the line (but not on it) also reveal a depression in the clay surface in the area around coordinate 18.3 km (Friborg and Thomsen, 1999), as seen on the few uncoupled GEOTEM soundings from that area. The layers above the heavy clay are interpreted to be the various sandy and clayey Quaternary and Tertiary sediments corresponding to the log in Figure 1. The individual formations cannot be distinguished with either the ground-based data or airborne data.

Correlation of the GEOTEM few-layer and multilayer inversions with the ground-based results gives only little information on the validity of the inversion of the airborne data. The main depth interval of investigation of the PROTEM 47 is within the first 100 m because almost all inversions have leveled off to a homogeneous half-space at this depth. The GEOTEM system has only very limited resolution in the top 100 m, as shown with the synthetic examples.

However, the comparison with a ground-based system highlights the differences in resolution capability. PROTEM 47 data can resolve between two and five layers, whereas the GEOTEM system only resolves three layers as a maximum. The multilayer inversion of GEOTEM data has more structural information in the top layers than does the few-layer inversion, in agreement with observations on the synthetic data.

The average resistivity of the CDT profile agrees with the the nonlinear inversion in the top 200 m. The only subsection with direct similarities is the deep conductor around coordinate 23–25 km, but the capacitive coupling around 24 km (Figure 8) might be responsible for the feature in the CDT profile. The conductive top layer from profile coordinate 15–22 km is also believed to be a coupling effect. It has been shown that unstable deconvolution of slightly noisy data leads to false indications of both poor and good conductors (Macnae et al., 1998). The feature around 15–22 km is also reflected in the PROTEM 47 section (Figures 9c, e), suggesting that these data are also affected by coupling. However, to positively identify a coupling, we need densely sampled profile data, which is not the case with the PROTEM 47 data, collected at approximately every 250 m.

For the rest of the profile, there are still prominent differences between the nonlinear inversions and the CDT. An example is seen around profile coordinates 6–10 km where the CDT has a near-surface conductive feature overlying a higher resistivity, whereas the opposite is the case for the few-layer and multilayer models.

DISCUSSION

Computation

Until recently, computation time has been critical in doing quantitative interpretation of extensive airborne data sets. As far as 1D models are concerned, this is no longer a severe limitation using modern fast PCs, but 1D interpretation brings new problems into focus. The GEOTEM system samples continuously in both on- and off-time, but the details of the resolution improvements obtained by including on-time data has not yet been quantified. Recent investigations, although incomplete, have indicated near-surface resolution improvements, which is not surprising (Christiansen and Christensen, 2001).

Transmitter waveform

Effersø et al. (1999) demonstrated the necessity of including the full system response in the calculation of responses from low-current ground-based methods. This was realized by using the transmitter waveform (nominal or measured close to the transmitter) and by modeling the effect of the filters of the receiver system. For airborne systems, it is preferable to use the transmitter waveform as measured by the receiver, because it encompasses all the effects of the system, including the effect of the induced currents in the aircraft, and, ideally, a program capable of on-time modeling is needed to extract the maximum amount of information.

Coupling to man-made conductors

Coupling is a serious problem when measuring in populated areas and has to be removed before interpretation. If not removed, the inversion can be erroneous, and a parameter analysis will be misleading. Removing coupled data is manual work and very time consuming. Hence, both clients and contractors must understand that the expenses of interpretation and evaluation of airborne data measured in populated areas are comparable to the survey expenses. An automated procedure identifying and removing coupled data sets is desirable, though it is must be expected that a fail-safe procedure is not likely to be found and that manual intervention will always be needed. Programs capable of simultaneously displaying data profiles, individual soundings, the flight video, and a map of the survey location would be helpful.

New strategies

The FA data used in this paper are calculated using the poststack x, y, and z-component data. A better solution would be calculation of a prestack FA, with subsequent stacking as a fourth data type. This procedure would need to be incorporated in the survey design, because at present only poststack values

are saved. This procedure would further reduce the effective noise on the FA data.

There is a need for more detailed noise description on airborne TEM data. At the moment no specific information on the noise is available. We suggest the following two procedures to be incorporated in the survey design:

1) Measurements at high altitude with the transmitter turned on. This is standard procedure today, but the time series must be stored and saved to enable a determination of not only average waveform but also its variability.
2) Measurement at survey altitude with the transmitter turned off, to estimate the ambient noise at the location. Again, full time series are needed.

The sum of the noise estimated from the two contributions would be a good approximation to the total noise.

CONCLUSIONS

Airborne TEM data can be interpreted with success using full nonlinear 1D inversion techniques. Joint inversion of the x- and z-component data turned out disadvantageous compared to the newly proposed strategy using the FA.

Interpretations and analyses of synthetic models show that airborne data can resolve up to three layers in a geophysical model. Ground-based methods resolve three (or more) layers in most cases. However, the depth of investigation is larger for the GEOTEM system than for the PROTEM 47 system. These observations are supported by the field data.

The main obstacle in an interpretation of field data is coupling affecting up to 70% of the measurements in a densely populated area like Denmark. If not identified and removed before interpretation they will result in erroneous models.

ACKNOWLEDGMENTS

Ringkjøbing County made the airborne and ground-based data available and were supportive in all matters. Without their help, this article would not have been written. Rambøll and Fugro Airborne Surveys were very helpful when asked about survey or system details. Lene Hjelm Poulsen participated in numerous helpful discussions concerning inversion and interpretation of both the airborne and ground-based data. We also thank Colin Farquharson, Peter Wolfgram, an anonymous reviewer, and associate editor Randall Mackie for their helpful comments.

REFERENCES

Annan, A. P., Smith, R. S., Lemieux, J., O'Connell, M. D., and Pedersen, R. N., 1996, Resistive-limit, time-domain AEM apparent conductivity: Geophysics, **61**, 93–99.

Christensen, N., 1990, Optimized fast Hankel transform filters: Geophys. Prosp., **38**, 545–568.

———2002, A generic 1-D imaging method for transient electromagnetic data, Geophysics, **67**, 438–447.

Christensen, N. B., and Auken, E., 1992, Simultaneous electromagnetic layered model analysis: Geoskrifter **41**, 49–56.

Christensen, N. B., and Sørensen, K. I., 1998, Surface and borehole electric and electromagnetic methods for hydrogeological investigations: Eur. J. Environmental and Eng. Geophys., **3**, 75–90.

Christensen, N. B., Sørensen, K. I., Christiansen, A. V., Rasmussen, T. M., and Poulsen, L. H., 2000, The use of airborne electromagnetic systems for hydrogeological investigations: Proc. Symp. on the Application of Geophysics to Environmental and Engineering Problems (SAGEEP), 73–82.

Christiansen, A. V., and Christensen, N. B., 2000, The sensitivity functions of TEM methods: 6th Mtg., Environmental and Engineering Geophys. Soc. Euro. Section, Proc., EM09.

———2001, Quantitative interpretation and analysis of airborne transient electromagnetic data in Denmark: 7th Mtg., Environmental and Engineering Geophys. Soci. Euro. Section, Proc., 122–123.

DeMoully, G. T., and Becker, A., 1984, Automated interpretation of airborne electromagnetic data: Geophysics, **49**, 1301–1312.

Effersø, F., Auken, E., and Sørensen, K. I., 1999, Inversion of band-limited TEM responses: Geophys. Prosp., **47**, 551–564.

Fitterman, D. V., and Stewart, M. T., 1986, Transient electromagnetic sounding for groundwater: Geophysics, **51**, 995–1005.

Friborg, R., and Thomsen, S., 1999, Kortlægning af Ribe Formationen. Et fællesjydsk grundvandssamarbejde [Mapping the Ribe Formation. A cooperate groundwater investigation project]: Ribe, Ringkjøbing, Viborg, Århus, Vejle og Sønderjyllands Amt Populær rapport.

Friis, H., Mikkelsen, J., and Sandersen, P., 1998, Depositional environment of the Vejle Fjord Formation, upper Oligocene–lower Miocene, Denmark: A barrier island/barrier protected depositional complex: Sedimentary Geol., **117**, 221–244.

Knight, J. H., and Raiche, A., 1982, Transient electromagnetic calculations using the Gaver-Stehfest inverse Laplace transform method: Geophysics, **47**, 47–50.

Liu, G., and Asten, M. W., 1993, Conductance-depth image of airborne TEM data: Expl. Geophys., **24**, 655–662.

Macnae, J., King, A., Stolz, N., Osmakoff, A., and Blaha, A., 1998, Fast AEM data processing and inversion, Expl. Geophy., **29**, 163–169.

Macnae, J., and Lamontagne, Y., 1987, Imaging quasi-layered conductive structures by simple processing of transient electromagnetic data: Geophysics, **52**, 545–554.

Macnae, J. C., Smith, R., Polzer, B. D., Lamontagne, Y., and Klinkert, P. S., 1991, Conductivity-depth imaging of airborne electromagnetic step-response data: Geophysics, **56**, 102–114.

McNeill, J. D., 1990, Use of electromagnetic methods for groundwater studies *in* Ward, S. H., Ed., Geotechnical and environmental geophysics: Soci. Expl. Geophys., 191–218.

Menke, W., 1989, Geophysical data analysis, rev. edn.: Discrete inverse theory: Academic Press Inc.

Munkholm, M. S., and Auken, E., 1996, Electromagnetic noise contamination on transient electromagnetic soundings in culturally disturbed environments: J. Environmental and Eng. Geophys., **1**, 119–127.

Nabighian, M. N., and Macnae, J. C., 1987, Time domain electromagnetic prospecting methods, *in* Nabighian, M. N., Ed., Electromagnetic methods in applied geophysics: Soc. Expl. Geophys., 427–520.

Pedersen, R., and Thompson, S., 1991, GEOTEM case history: Appendix G of "Time domain electromagnetic prospecting methods" by M. N. Nabighian and J. C. Macnae, *in* Nabighian, M. N., Ed., Electromagnetic methods in applied geophysics: Soc. Expl. Geophys., 509–513.

Poulsen, L. H., and Christensen, N. B., 1998, Hydrogeophysical mapping with the transient electromagnetic sounding method: Eur. J. of Environmental and Eng. Geophys., **3**, 201–220.

Poulsen, L. H., 2000, Inversion of airborne transient electromagnetic data: Geological Survey of Denmark and Greenland, Ministry of Environment and Energy, Rapport, 2000/82.

Smith, R. S., 2000, The realizable resistive limit: A new concept for mapping geological features spanning a broad range of conductances, Geophysics: **65**, 1124–1127.

——— 2001a, On removing the primary field from fixed-wing time-domain airborne electromagnetic data: Some consequences for quantitative modelling, estimating bird position and detecting perfect conductors: Geophys. Prosp., **49**, 405–416.

——— 2001b, Tracking the transmitting-receiving offset in fixed-wing transient EM systems: Methodology and applications, Expl. Geophys., **32**, 14–19.

Smith, R. S., and Balch, S. J., 2000, Robust estimation of the band-limited inductive-response from impulse-response TEM measurements taken during the transmitter switch-off and the transmitter off-time: Theory and an example from Voisey's Bay, Labrador, Canada: Geophysics, **65**, 476–481.

Smith, R. S., and Keating, P. B., 1996, The usefulness of multicomponent, time-domain airborne electromagnetic measurements, Geophysics, **61**, 74–81.

Smith, R. S., and Lee, T. J., 2002, Using the moments of a thick layer to map the conductance and conductivity from airborne electromagnetic data: J. Appl. Geophys., **49**, 173–183.

Sørensen, K. I., 1995, Pulled array continuous vertical electrical sounding (PA-CVES): Proc. Symp. on the Application of Geophysics

to Environmental and Engineering Problems (SAGEEP), 893–898.
Sørensen, K. I., Auken, E., and Thomsen, P., 2000, TDEM in groundwater mapping—A continuous approach.: Proc. Symp. on the Application of Geophysics to Environmental and Engineering Problems (SAGEEP), 485–491.
Sørensen, K., Thomsen, P., Auken, E., and Pellerin, L., 2001, Effect of coupling in electromagnetic data: 7th Mtg., Environmental and Eng. Geophys. Soc. Euro. Section, Proc., 108–109.
Stolz, E. M., and Macnae, J. C., 1998, Evaluating EM waveforms by singular-value decomposition of exponential basis functions: Geophysics, **63**, 64–74.
Wolfgram, P., and Karlik, G., 1995, Conductivity-depth transform of GEOTEM data: 13th Geophys., Conf., Australian Soc. Expl. Geophys., Proc., 179–185.